Available online at www.sciencedirect.com
ScienceDirect
Journal of Power Sources 162 (2006) 629–635
JOURNAL OF POWER SOURCES
www.elsevier.com/locate/jpowsour

The effects of extra Li content, synthesis method, sintering temperature on synthesis and electrochemistry of layered $LiNi_{1/3}Mn_{1/3}Co_{1/3}O_2$

Lianqi Zhang [a,*], Xiaoqing Wang [a], Takahisa Muta [a], Decheng Li [a], Hideyuki Noguchi [a], Masaki Yoshio [a], Renzhi Ma [b], Kazunori Takada [b], Takayoshi Sasaki [b]

[a] *Department of Applied Chemistry, Saga University, Saga 840-8052, Japan*
[b] *Advanced Materials Laboratory, National Institute for Materials Science, Namiki 1-1, Tsukuba, Ibaraki 305-0044, Japan*

Received 22 December 2005; received in revised form 29 June 2006; accepted 30 June 2006
Available online 1 September 2006

Abstract

The effects of extra Li content, different synthesis method and sintering temperature on synthesis, structure and electrochemistry of $LiCo_{1/3}Ni_{1/3}Mn_{1/3}O_2$ were investigated. It was shown that extra Li content, homogeneous precursor and a high sintering temperature contributed to the formation of single phase compound. Extra Li content not only accelerated formation of pure phase due to effectively suppressing development of NiO impurity, but also brought about considerable variations in electrochemistry. In the case of $x = 1.3$ (the molar ratio of Li versus M ($M = Co_{1/3}Ni_{1/3}Mn_{1/3}$) at starting materials), a plateau-like stage at >4.3 V during the initial charge process was apparently observed, accompanying a remarkably improved initial charge capacity. Different precursors derived from different synthesis methods caused the impressive differences in electrochemistry of $LiCo_{1/3}Ni_{1/3}Mn_{1/3}O_2$. Homogeneous precursors derived from spray-drying method resulted in significantly improved electrochemical performances in contrast with ones obtained by direct decomposition of acetates and even subsequent ball-milling. This may be related to the reduced occupancy of transitional metal ions in Li layers, smaller particles size and possibly good material homogeneity in $LiCo_{1/3}Ni_{1/3}Mn_{1/3}O_2$.

Keywords: Lithium ion batteries; $LiCo_{1/3}Ni_{1/3}Mn_{1/3}O_2$; Extra Li content; Synthesis method; Spray-drying

1. Introduction

There is an expanding demand for lithium ion batteries as power sources for portable electronic equipments, such as cellular phone, camcorder and laptop computer; in future, the batteries will be scaled-up in view of their use in electric vehicles and energy storage. Cathode materials play an important role on determining performances of lithium ion batteries. Currently, $LiCoO_2$ are widely commercialized as a cathode material in lithium ion batteries; however, its relatively high cost inhibits its further use in price-sensitive applications, such as electric vehicles. Therefore, search for an alternative cathode material, superior to $LiCoO_2$ in view of capacity, economy, non-toxicity and safety, is still ongoing task.

During the search for such an improved cathode material, layered $LiCo_{1/3}Ni_{1/3}Mn_{1/3}O_2$ with the performances comparable to or better than $LiCoO_2$, recently attracted intense attention [1–11]. In this material, Ni, Mn and Co exist as 2+, 4+ and 3+ oxidation states, respectively, which is opposite to the conventional wisdom that Ni is 3+ in $LiNiO_2$ and a lot of Ni^{2+} can result in vitally detrimental effects to electrochemical performances. Ni and Co acts as the electrochemically active species during cycling in the voltage range of >2.5 V, while Mn^{4+} is electrochemically inert and functions as stable framework. We recently developed a spray-drying method to produce excellent $LiCo_{1/3}Ni_{1/3}Mn_{1/3}O_2$ and found that synthesis method had an important impact on electrochemical

* Corresponding author. Present address: Advanced Materials Laboratory, National Institute for Materials Science, Namiki 1-1, Tsukuba, Ibaraki 305-0044, Japan. Tel.: +81 29 851 3354x8643; fax: +81 29 854 9061.
E-mail address: lianqi.zhang@nims.go.jp (L. Zhang).

0378-7753/$ – see front matter © 2006 Elsevier B.V. All rights reserved.
doi:10.1016/j.jpowsour.2006.06.089

performances [11]. It was observed in the investigation that pure $LiCo_{1/3}Ni_{1/3}Mn_{1/3}O_2$ can be hardly prepared at the same sintering condition of 900 °C using a simple combustion method of acetates despite of its simplicity and expectable economical merit; NiO as an impure phase with rock salt structure separated from layered main phase, possibly due to inhomogeneous distribution of Ni, Co, Mn. In the case, it can be imagined that no Li salt should stay around or closely from NiO; otherwise, $Li_zNi_{2-z}O_2$ ($0 < z \leq 1$) having gradually enhanced ordering structure with increasing z value (at $z = 1$, it is a nearly ideal layered structure of $LiNiO_2$) possibly forms. Therefore, it can be expected that adding excess Li salt at starting materials should help to suppressing or refraining formation of NiO and, instead, developing $Li_zNi_{2-z}O_2$ ($0 < z \leq 1$) phase that may better favors formation of solid solution with other layered components to a single phase because of their structural similarity. This will be effectively verified in the current work. In fact, it has been already claimed that extra Li^+ ($y > 0$ in $Li_{1+y}(Ni_{1/3}Mn_{1/3}Co_{1/3})_{1-y}O_2$) can be incorporated into transitional metals layers in $LiCo_{1/3}Ni_{1/3}Mn_{1/3}O_2$, accompanying the oxidization of partial Ni^{2+} to Ni^{3+} to maintain a single phase compound [9,10]. Similar phenomenon was also reported in $LiNiO_2$ and $LiNi_{1/2}Mn_{1/2}O_2$ [12–14]. In the references [9,10], the investigations were mainly focused on the effect of extra Li content on electrochemistry of the $LiCo_{1/3}Ni_{1/3}Mn_{1/3}O_2$, which were prepared at a same high sintering temperature, such as 900 °C using extra Li content at starting materials up to the 1.2 molar ratio of Li versus total transitional metals. However, the effect of extra Li on synthesis, structure and electrochemistry in a larger range under different sintering temperatures is still not much clear in $LiCo_{1/3}Ni_{1/3}Mn_{1/3}O_2$. In combination with one recent report on solid solution in the system of $LiNiO_2$–$LiCoO_2$–Li_2MnO_3 (or $LiNi_{1-z}Co_zO_2$–Li_2MnO_3) [15], the nature of the materials with extra Li content can be further shed light on. Theoretically, an excess Li with $y = 1/7$ in $Li_{1+y}(Ni_{1/3}Mn_{1/3}Co_{1/3})_{1-y}O_2$ can be incorporated into transitional metals sites, along with transformation of all Ni^{2+} to Ni^{3+} in $LiCo_{1/3}Ni_{1/3}Mn_{1/3}O_2$ and formation of $Li[Li_{1/7}Co_{2/7}Ni_{2/7}Mn_{2/7}]O_2$. Actually, $Li[Li_{1/7}Co_{2/7}Ni_{2/7}Mn_{2/7}]O_2$ can be prepared and considered as one member of solid solutions of $LiNiO_2$–$LiCoO_2$–Li_2MnO_3 (or $LiNi_{1-z}Co_zO_2$–Li_2MnO_3) according to the recent report [15], because it can be reformulated as $2/7LiNiO_2 \cdot 2/7LiCoO_2 \cdot 3/7Li[Li_{1/3}Mn_{2/3}]O_2$. Therefore, the materials prepared using extra Li content may be considered as the members of solid solution series between $LiCo_{1/3}Ni_{1/3}Mn_{1/3}O_2$ and $Li[Li_{1/7}Co_{2/7}Ni_{2/7}Mn_{2/7}]O_2$. Some clues in our current report can be found to support the assumption above.

In this work, following our previous work [11], we report the synthesis of $LiNi_{1/3}Mn_{1/3}Co_{1/3}O_2$ cathode materials under different conditions. The effects of different Li content (the molar ratio of Li versus M ($M = Co_{1/3}Ni_{1/3}Mn_{1/3}$) at starting materials ranged from 1.0 to 1.3), sintering temperature and synthesis method on synthesis, structure and electrochemical performances were examined in detail. The more reasonable explanation for good electrochemical performances of the best sample prepared by spray-drying method was proposed in combination with further structural analysis and morphology characterization.

2. Experimental

$LiNi_{1/3}Mn_{1/3}Co_{1/3}O_2$ was firstly prepared by direct decomposition of acetates at 400 °C, followed by heating at different higher temperatures for 20 h after grinding (method A). With this method, different Li contents at starting materials, ranging from 1.0 to 1.3 in molar ratio of Li versus M ($M = Ni_{1/3}Mn_{1/3}Co_{1/3}$) and represented as x below, were adopted to investigate the effect of extra-Li effect on synthesis and electrochemical performances of $LiNi_{1/3}Mn_{1/3}Co_{1/3}O_2$. In order to investigate effect of different synthesis method on $LiNi_{1/3}Mn_{1/3}Co_{1/3}O_2$, ball-milling (method B) and spray-drying (method C) methods were also employed to prepare $LiCo_{1/3}Ni_{1/3}Mn_{1/3}O_2$. For ball-milling method, the mixture after decomposition of acetates was subject to ball-milling for 1 h and then calcined at different higher temperatures for 20 h. For spray-drying method, samples were prepared as the procedure below. Stoichiometric $LiNO_3$, $M(CH_3COO)_2 \cdot 4H_2O$ (M = Ni, Co and Mn) were dissolved in water. The transparent solution was fed into a spray-drying instrument (pulvis mini-spray GB22, Yamato, Japan) to produce homogenous precursors. The precursors were initially heated at 300 °C in air and then calcined at different higher temperatures for 20 h after grinding.

The crystallographic properties of samples were characterized using a Rigaku diffractometer (RINT 1000) with Cu Kα radiation. Structure parameters for several samples were refined by a Rietveld method using a computer program (RIETAN) [16] on the basis of α-$NaFeO_2$-type structure with space group *R*-3*m*. A virtual chemical species representing the transition metal elements in samples, M, was used in the refinement. It has the mean scattering amplitude of the transition metal elements. Li, M and O were distributed to 3*a* (0, 0, 0), 3*b* (0, 0, 1/2) and 6c (0, 0, *z*) sites, respectively. Total occupancy of each site was constrained to be unity. Li and M were allowed to exchange during refinement. The *R* factors obtained in the refinement on these samples (e.g. R_{wp} is about 10%) were comparable to the reported values in $LiNi_xMn_xCo_{1-2x}O_2$ ($0 \leq x \leq 0.5$) [3]. The scan electron microscope (SEM) images were obtained by JEOL JSM-5200 electron microscope.

The charge and discharge characteristics of Li–Ni–Mn–Co–O cathodes were examined in CR2032 coin-type half-cell (Li/Li–Ni–Mn–Co–O). Cells were composed of a cathode and a lithium metal anode (Cyprus Foote Mineral Co.) separated by a porous polypropylene film (Celgard 3401) and two glass fiber mats. The cathode consisted of 20 mg active material and 12 mg conductive binder (8 mg polytetrafluoroethylene (PTFE) and 4 mg acetylene black). It was pressed on a stainless steel mesh at 800 kg cm^{-2} and then dried in vacuum at 170 °C for 5 h. The electrolyte solution was a 1:2 mixture of ethylene carbonate (EC) and dimethylcarbonate (DMC) in volume containing 1 M $LiPF_6$. All cells were assembled in an argon-filled dry box. Cells were cycled in such a way (CCCV) that they were charged to 4.5 V at a constant current density of 0.2 mA cm^{-2} (20 mA g^{-1}) and then

kept at 4.5 V for 3 h, followed by being discharged to 3.0 V at a constant current density of 0.2 mA cm^{-2} (20 mA g^{-1}). For the measurement of rate capability, charge process was executed in CCCV mode at a constant current density of 0.2 mA cm^{-2} (20 mA g^{-1}), but discharge process went on at different rates.

3. Results and discussion

Fig. 1 shows XRD profiles of $LiCo_{1/3}Ni_{1/3}Mn_{1/3}O_2$ prepared by the direct decomposition of acetates using different Li contents at starting materials under different temperatures. At 800 °C, the samples with $x = 1.0$ and 1.1 were apparently the mixture, while extra Li with $x = 1.2$ and 1.3 made a single phase compound indexable to a layered α-$NaFeO_2$-type structure (space group *R*-3*m*, no. 166), despite that the splitting of 0 0 6 and 1 0 2 as well as 1 0 8 and 1 1 0 reflections was not developed well in comparison with the samples prepared at a higher temperature. With careful identification, three phases, cubic NiO, layered Li_2MnO_3 and, possibly, layered $Li_z(NiCoMn)_{2-z}O_2$ were developed in the case of $x = 1.0$ and 1.1, as marked in figure. By contrast with $x = 1.0$, increasing Li content up to $x = 1.1$ indeed reduced the formation of cubic NiO according to intensity change of the diffraction peak at around 44° and also increased the Li_2MnO_3 content in the mixture; when *x* increased to 1.2, NiO phase disappeared, accompanying the formation of a single phase. Therefore, the disappearance of NiO phase is possibly an indicator that a pure phase can be observed. At 900 °C, a weak reflection coming from NiO impurity was still detected only in the sample with $x = 1.0$. The splitting of 006 and 102 as well as 108 and 110 reflections became clear with increasing Li content. At 950 °C, all samples presented a single phase compound with well-developed XRD patterns. As a result, extra Li content at starting materials can apparently accelerate the formation of single phase compound. It is possibly due to the mechanism mentioned in the introduction that rock-salt-structured NiO phase is structurally incompatible with layered structure and its formation is suppressed as extra Li content at starting materials was added, accompanying the development of layered-ordering $Li_zNi_{2-z}O_2$ and further solid solution with other layered components to produce a layered single phase. Furthermore, extra Li also appeared to benefit development of layered structure according to the splitting of 0 0 6 and 1 0 2 as well as 1 0 8 and 1 1 0 reflections. In addition, an enough high sintering temperature also evidently played a key role on formation of pure phase compound. With careful observation, some weak and broad reflections at around 21° for the samples prepared with large *x* values were detected at low temperatures (800 and 900 °C), which are usually ascribed to short-range supper lattice order of Li and transitional metals in the transitional metals-containing layers [17] and supports that extra Li^+ are really incorporated into transitional metals sites, but they became negligible at 950 °C.

Slight and regular shifts in some diffraction peaks can be detected due to different Li contents at starting materials and sintering temperatures. This can be reflected by their lattice parameters as shown in Table 1. Lattice parameters, *a* and *c*, monotonously decreased with increasing Li content for the samples prepared at the same temperature, as shown in Fig. 2. When extra Li^+ are incorporated into the sites of transitional metals layers in $LiCo_{1/3}Ni_{1/3}Mn_{1/3}O_2$, the formation of partial Ni^{3+} to maintain a single phase compound is accompanied; as *x* increases to 1.33, all Ni^{2+} transform to Ni^{3+} and $Li[Li_{1/7}Co_{2/7}Ni_{2/7}Mn_{2/7}]O_2$ forms. Thus, the materials prepared with different Li contents, as discussed previously, may be considered as solid solution between $LiCo_{1/3}Ni_{1/3}Mn_{1/3}O_2$ and

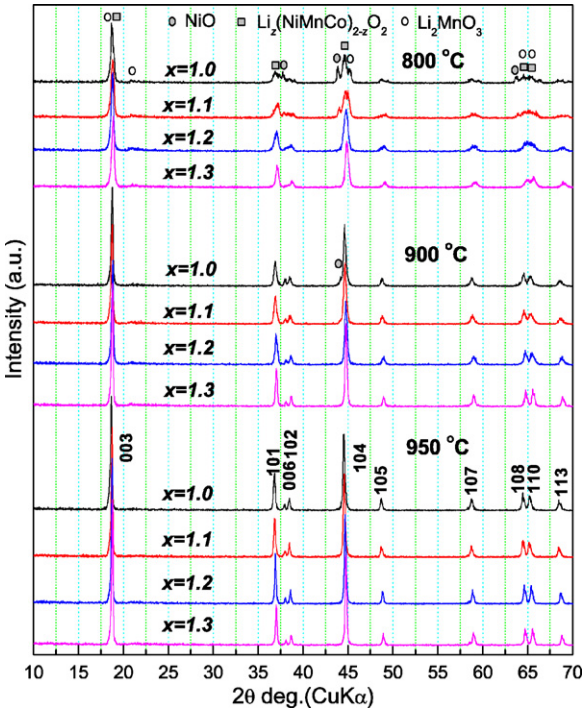

Fig. 1. XRD patterns of $LiCo_{1/3}Ni_{1/3}Mn_{1/3}O_2$ prepared by the direct decomposition of acetates (method A) using different Li contents under different sintering temperatures.

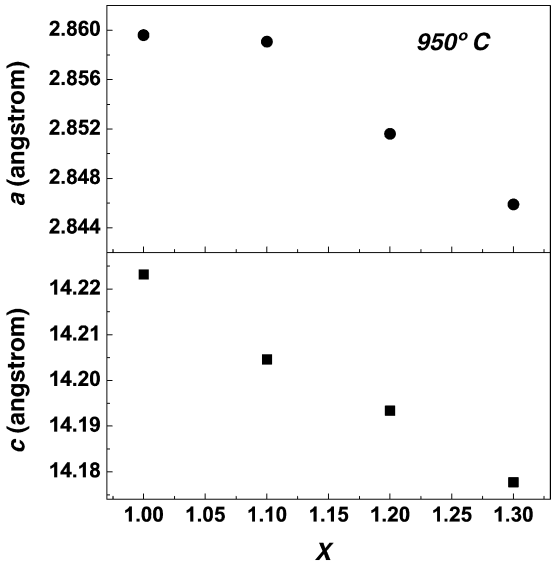

Fig. 2. The change in lattice parameters, *a* and *c*, with increasing *x* (Li content at starting materials) for $LiCo_{1/3}Ni_{1/3}Mn_{1/3}O_2$ prepared by the direct decomposition of acetates (method A) using different Li contents at 950 °C.

Table 1
Lattice parameters, initial charge, discharge and irreversible capacities for $LiCo_{1/3}Ni_{1/3}Mn_{1/3}O_2$ prepared by the direct decomposition of acetates (method A) using different Li contents under different sintering temperatures

Samples	Lattice parameters		Charge capacity (mAh g^{-1})	Discharge capacity (mAh g^{-1})	Irreversible capacity (mAh g^{-1})
	a (Å)	c (Å)			
800 °C					
$x = 1.1$			160.7	131.3	29.4
$x = 1.2$	2.8447	14.1438	172.6	137.4	34.5
$x = 1.3$	2.8411	14.1160	194.7	140.9	54.7
900 °C					
$x = 1.0$	2.8548	14.2040	190.1	155.2	34.9
$x = 1.1$	2.8542	14.1937	197.1	163.2	34.0
$x = 1.2$	2.8469	14.1712	183.2	152.0	31.2
$x = 1.3$	2.8448	14.1709	216.8	156.5	60.3
950 °C					
$x = 1.0$	2.8596	14.2232	201.1	167.4	33.7
$x = 1.1$	2.8591	14.2046	206.1	169.8	36.3
$x = 1.2$	2.8516	14.1934	200.3	167.2	33.1
$x = 1.3$	2.8459	14.1777	225.0	173.1	52.0

$Li[Li_{1/7}Co_{2/7}Ni_{2/7}Mn_{2/7}]O_2$, which can be supported by the gradual change in lattice parameters, a and c, with increasing x value, as shown in Fig. 2. The real compositions of the compounds should lie in the range of $Li_{1+y}(Ni_{1/3}Mn_{1/3}Co_{1/3})_{1-y}O_2$ ($0 \le y \le 1/7$). The solid solution series have such a substitution equation: $Co^{3+} + 7Ni^{2+} + Mn^{4+} = 3Li^{+} + 6Ni^{3+}$. The ionic radii of Li^+, Ni^{2+}, Ni^{3+}, Co^{3+} and Mn^{4+} are 0.76, 0.69, 0.56, 0.53 and 0.54 Å, respectively [18]; hence, the average ionic radius of $[3Li^+ + 6Ni^{3+}]$ is smaller than that of $[Co^{3+} + 7Ni^{2+} + Mn^{4+}]$ (0.627 and 0.656 Å, respectively). As a result, the smaller mean ionic radius causing the shrinkage of the transitional metal layers may mainly account for the shrinkage in a- and c-axes with increasing x. Additionally, the samples prepared with the same Li content at a higher temperature appeared to present the slight expansion in a- and c-axes in contrast to those prepared at a lower temperature. This is possibly related to the formation of lower valence M, like Ni^{2+} in the sample at a higher temperature (impure phases, trace amount of Li_2O and Li_2CO_3, possibly appear in this case, but are impossible to be detected by XRD) than at a lower temperature, because a higher temperature usually benefits the formation of low valence [19].

Fig. 3 shows XRD patterns of $LiCo_{1/3}Ni_{1/3}Mn_{1/3}O_2$ prepared via different precursors derived from different methods. $LiCo_{1/3}Ni_{1/3}Mn_{1/3}O_2$ prepared via method A, A900 (final heating at 900 °C) and A950 (final heating at 950 °C), indicated that a temperature of ≥950 °C can cause a pure phase compound. Whereas the samples prepared via method B, B800 (final heating at 800 °C) and B900 (final heating at 900 °C), indicated that $LiCo_{1/3}Ni_{1/3}Mn_{1/3}O_2$ could be obtained at 900 °C. In contrast, the samples prepared via mehod C, C800 (final heating at 800 °C) and C900 (final heating at 900 °C), showed that $LiCo_{1/3}Ni_{1/3}Mn_{1/3}O_2$ can be obtained at a lower temperature of 800 °C. Spray-drying (method C) is a good way to produce the precursors with homogeneity at an atomic scale [20]. Ball-milling is also helpful to enhance the homogeneity of precursors. As a result, it can be believed that the homogeneous precursors can accelerate the formation of $LiCo_{1/3}Ni_{1/3}Mn_{1/3}O_2$.

Fig. 4 shows the charge–discharge curves and cycling performance of $LiCo_{1/3}Ni_{1/3}Mn_{1/3}O_2$ prepared by the direct decomposition of acetates (method A) using different Li contents at starting materials under different sintering temperatures. It is clear that sintering temperature had an apparent effect on initial charge and discharge capacities, that is, capacities increased with the increase in final heating temperature, as summarized in Table 1. Extra Li content brought about little change in capacity in the range of $x \le 1.2$ and a slight variation in charge–discharge curve that a plateau-like shape was developed at the high voltage range of initial change curve. However, the significant change was made in the case of $x = 1.3$. A remarkably improved initial charge capacity along with the prominent change in charge–discharge curves were observed with extra Li of $x = 1.3$, as indicated in Fig. 4. The sample presented an apparent plateau-like stage as the charge voltage was over 4.3 V, which was clearly reflected as a sharp shoulder

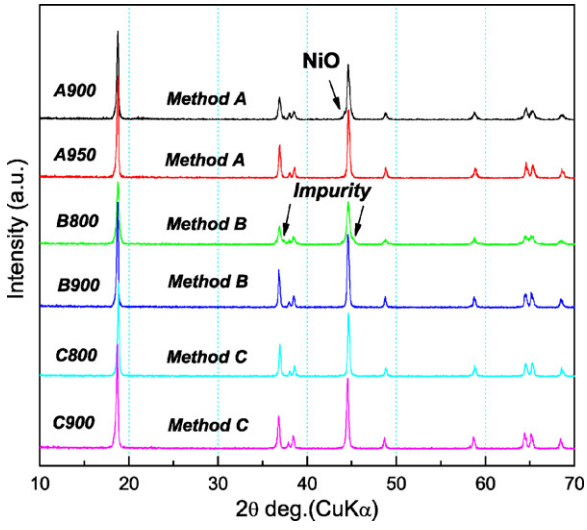

Fig. 3. XRD patterns of $LiCo_{1/3}Ni_{1/3}Mn_{1/3}O_2$ prepared via different methods under different sintering temperatures.

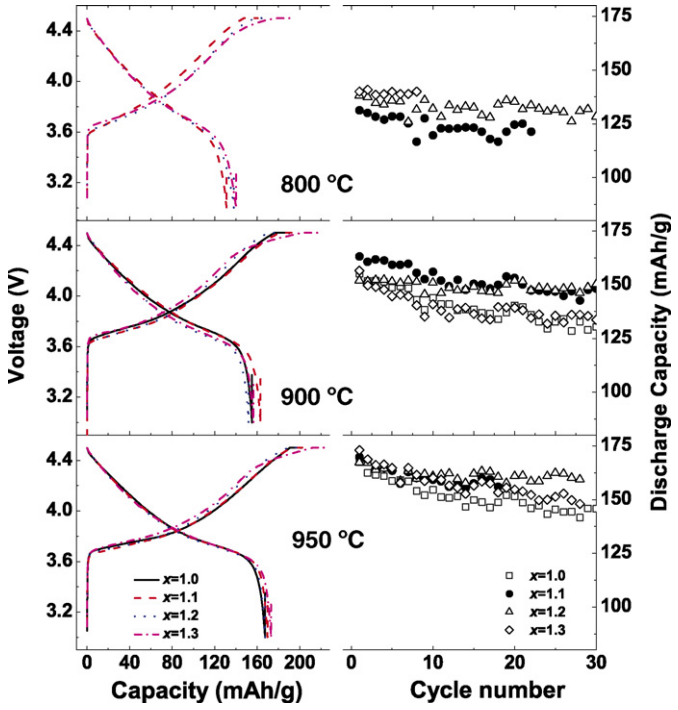

Fig. 4. Initial charge–discharge curves and cycling performance for $LiCo_{1/3}Ni_{1/3}Mn_{1/3}O_2$ prepared by the direct decomposition of acetates (method A) using different Li contents under different sintering temperatures.

of peak in the plots of differential capacity versus voltage, as shown in Fig. 5. This phenomenon was not found in references [9,10]. Enough high excess Li content at starting materials is necessary to clearly observe the phenomenon. The shoulder intensity decreased with decreasing Li content and disappeared at $x = 1.0$. It was reported that the simultaneous removal of Li and O from the structure in the similar layered compounds with extra Li^+ in transitional metals-containing layers can occur and bring about an irreversible plateau at about 4.5 V during initial charge process [17]. Similar phenomenon was also observed in the solid solution system of $LiNiO_2$–$LiCoO_2$–Li_2MnO_3 [15].

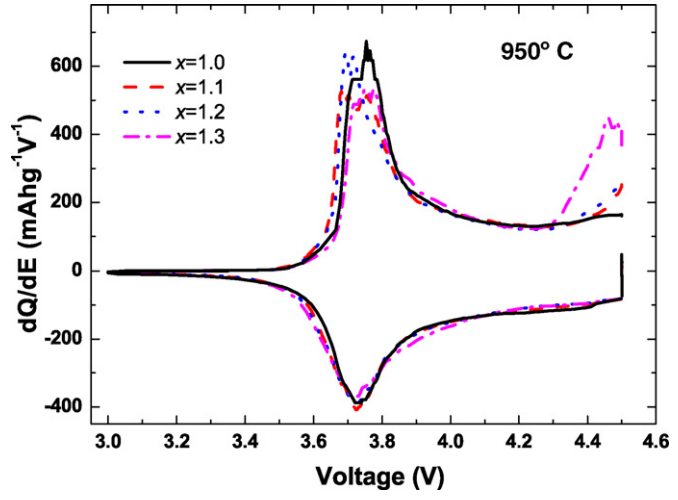

Fig. 5. The derivative plots obtained from charge–discharge curves for $LiCo_{1/3}Ni_{1/3}Mn_{1/3}O_2$ prepared by the direct decomposition of acetates (method A) using different Li contents at 950 °C.

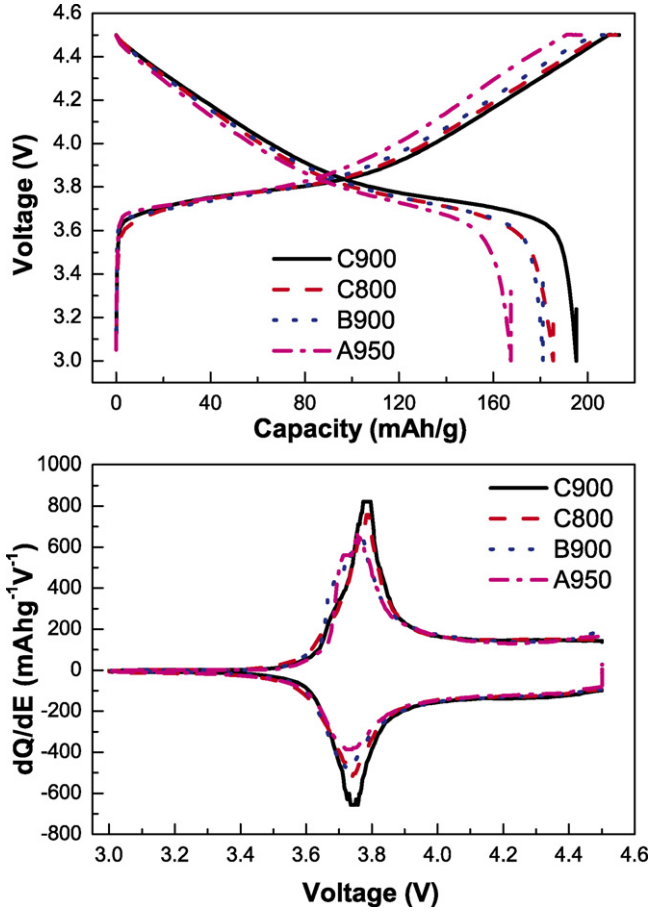

Fig. 6. Initial charge–discharge curves and their derivative plots for $LiCo_{1/3}Ni_{1/3}Mn_{1/3}O_2$ prepared via different methods.

As discussed above, the material with $x = 1.33$ having the nominal composition of $Li[Li_{1/7}Co_{2/7}Ni_{2/7}Mn_{2/7}]O_2$ is one member of $LiNiO_2$–$LiCoO_2$–Li_2MnO_3 solid solution system while the materials prepared with different Li contents can be considered as the solid solution between $LiCo_{1/3}Ni_{1/3}Mn_{1/3}O_2$ and $Li[Li_{1/7}Co_{2/7}Ni_{2/7}Mn_{2/7}]O_2$. Therefore, it is possible that the similar redox mechanism occurs in our samples prepared with extra Li content. In turn, the gradual change in electrochemistry, increasing shoulder in Fig. 5 with increasing x, also supported the assumption that the materials prepared using different Li content are solid solution series between $LiCo_{1/3}Ni_{1/3}Mn_{1/3}O_2$ and $Li[Li_{1/7}Co_{2/7}Ni_{2/7}Mn_{2/7}]O_2$. From the cycling data, the sample with $x = 1.2$ showed the best cycleability, as shown in Fig. 4.

Fig. 6 shows the charge–discharge curves and their derivative plots for $LiCo_{1/3}Ni_{1/3}Mn_{1/3}O_2$ prepared via different methods. All samples exhibited smooth charge–discharge curves, corresponding to a single peak at around 3.75 V as shown in the plots of differential capacity versus voltage. The sample prepared by method C at 900 °C (C900) showed the highest charge–discharge capacities and smallest irreversibility as summarized in Table 2. Despite the difference in initial charge–discharge capacities, similar cycleability was observed for these samples except for C800, as indicated in Fig. 7. Fig. 8 shows the comparative investigation on rate capability between the samples C900 and B900. The sample C900 produced much

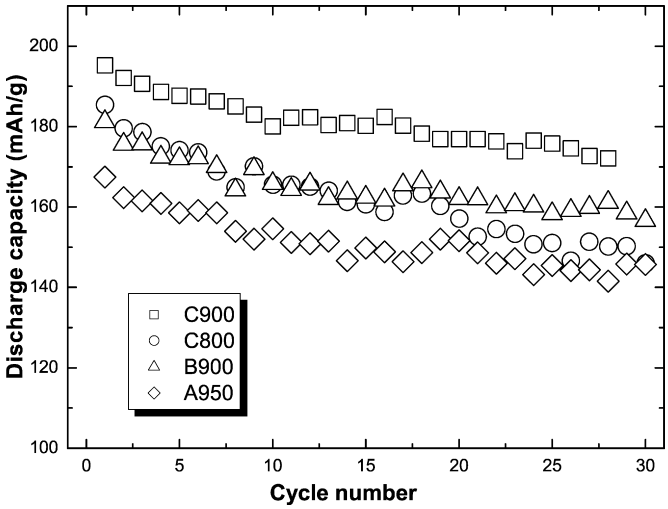

Fig. 7. The cycling performance of $LiCo_{1/3}Ni_{1/3}Mn_{1/3}O_2$ prepared via different methods.

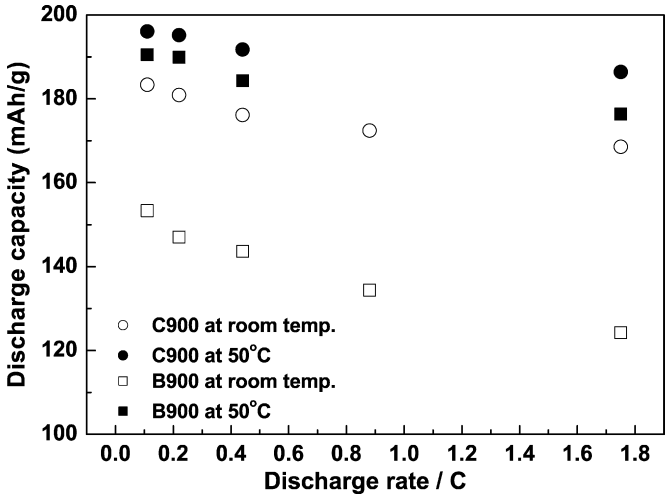

Fig. 8. Rate capabilities of samples C900 and B900 operated at room temperature and 50 °C.

better rate capability than B900 and temperature effect on rate capability for the sample C900 is much less than that for B900. Judging from initial charge–discharge capacities and rate capability, the preference of synthesis method followed such an order of C > B > A. The sample C900 is the most promising in view of its capacity, cycling performance and rate capability.

In order to clarify the origin of better performances of the sample C900, the further structural analysis by Rietveld refinement and morphology characterization by SEM were performed on these samples. The obtained lattice parameters, *a* and *c*, and occupancy of transitional metals ions in Li layers by Rietveld refinement were summarized in Table 2. The lattice parame-

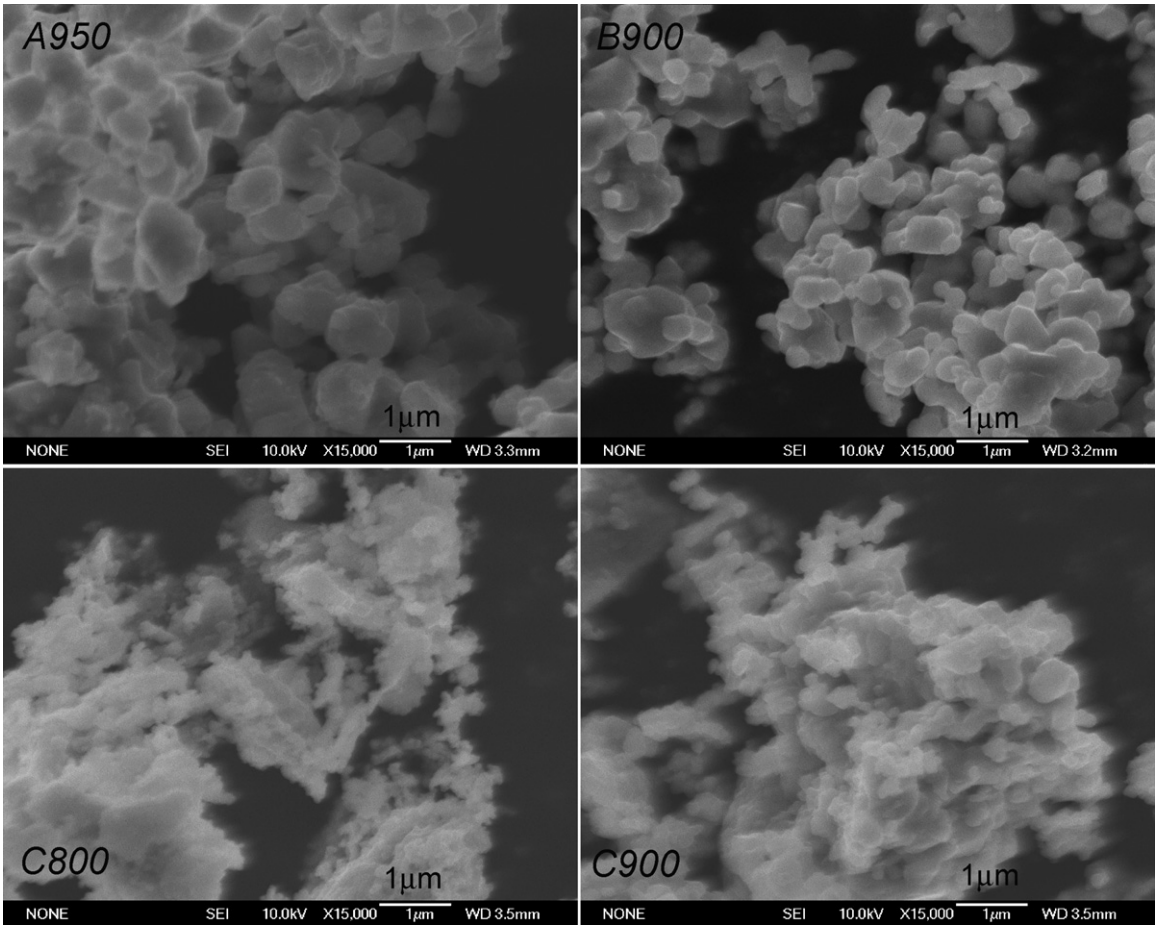

Fig. 9. SEM images of $LiCo_{1/3}Ni_{1/3}Mn_{1/3}O_2$ prepared via different methods.

Table 2
The obtained lattice parameters and occupancy of transitional metals ions M in Li layers by Rietveld analysis as well as initial charge, discharge and irreversible capacities for $LiCo_{1/3}Ni_{1/3}Mn_{1/3}O_2$ prepared via different methods

Samples	Lattice parameters		Occupancy of M in Li layers (%)	Charge capacity ($mAh\,g^{-1}$)	Discharge capacity ($mAh\,g^{-1}$)	Irreversible capacity ($mAh\,g^{-1}$)
	a (Å)	c (Å)				
A950	2.8634	14.2368	3.4	201.1	167.4	33.7
B900	2.8630	14.2353	3.3	213.1	181.2	31.9
C800	2.8623	14.2394	3.0	212.1	185.4	26.7
C900	2.8628	14.2438	2.0	213.5	195.3	18.2

ters, a and c, presented slight difference for those samples, but a difference in occupancy of transitional metal ions in Li layers was made. The occupancy of transitional metals ions in Li layers for the samples prepared by spray-drying method, especially for C900, showed a relatively low value. Fig. 9 shows the morphologies of four $LiCo_{1/3}Ni_{1/3}Mn_{1/3}O_2$ prepared via different methods. A950 and B900 had better-developed particles, the size of which ranged from about 0.5 to 1 μm. It seemed that A950 had a slightly larger particle size in comparison with B900. In contrast, the samples prepared by spray-drying method, C900 and C800, showed the smaller particle size, especially for C800. Some small particles in C900 seemed to be agglomerated into a large one with a second particle size of <1 μm, while C800 consisted of <200 nm particles. In summary, three factors including the reduced occupancy of transitional metals ions in Li layers, smaller particles size and possibly good homogeneity of materials may mainly account for the improved electrochemical properties for the C900 sample.

4. Conclusion

$LiCo_{1/3}Ni_{1/3}Mn_{1/3}O_2$ was prepared under various conditions. The effects of extra Li content at starting materials, sintering temperature and different precursors obtained from different synthesis methods on synthesis, structure and electrochemistry of $LiCo_{1/3}Ni_{1/3}Mn_{1/3}O_2$ were investigated. Extra Li content not only contributed to the formation of a single phase compound at a lower sintering temperature, but also caused the change in electrochemistry especially when the molar ratio of Li versus M ($M = Co_{1/3}Ni_{1/3}Mn_{1/3}$) reached 1.3. In the case of $x = 1.3$, the sample exhibited the remarkably improved initial charge capacity, accompanying the appearance of a plateau-like stage at >4.3 V. The materials prepared using different extra Li contents may be considered as the solid solution series between $LiCo_{1/3}Ni_{1/3}Mn_{1/3}O_2$ and $Li[Li_{1/7}Co_{2/7}Ni_{2/7}Mn_{2/7}]O_2$. Homogeneous precursors cannot only accelerate the formation of $LiCo_{1/3}Ni_{1/3}Mn_{1/3}O_2$, but also significantly improve the electrochemical performances. $LiCo_{1/3}Ni_{1/3}Mn_{1/3}O_2$ prepared at 900 °C via the precursors derived from spray-drying method showed the best electrochemical performances among the materials investigated in the current work. This may be related to the reduced occupancy of transitional metal ions in Li layers, smaller particles size and possibly good homogeneity of materials.

References

[1] T. Ohzuku, Y. Makimura, Chem. Lett. 7 (2001) 642.
[2] N. Yabuuchi, T. Ohzuku, J. Power Sources 119–121 (2003) 171.
[3] S. Jouanneau, D.D. Macneil, Z. Lu, S.D. Beattie, G. Murphy, J.R. Dahn, J. Electrochem. Soc. 140 (2003) A1299.
[4] Z. Lu, D.D. MacNeil, J.R. Dahn, Electrochem. Solid State Lett. 4 (2001) A200.
[5] I. Belharouak, Y.K. Sun, J. Liu, K. Amine, J. Power Sources 123 (2003) 247.
[6] K.M. Shaju, G.V. Subba Rao, B.V.R. Chowdari, Electrochim. Acta 48 (2002) 145.
[7] W. Yoon, C.P. Grey, M. Balasubramanian, X. Yang, D.A. Fisher, J. McBreen, Electrochem. Solid State Lett. 7 (2004) A53.
[8] Z. Wang, Y. Sun, L. Chen, X. Huang, J. Electrochem. Soc. 151 (2004) A914.
[9] J. Choi, A. Manthiram, Electrochem, Solid State Lett. 7 (2004) A356.
[10] Y.M. Todorov, K. Numata, Electrochim. Acta. 50 (2004) 495.
[11] D. Li, T. Muta, L. Zhang, M. Yoshio, H. Noguchi, J. Power Sources 132 (2004) 150.
[12] R. Stoyanova, E. Zhecheva, R. Alcantara, J.L. Tirado, G. Bromiley, F. Bromiley, T.B. Ballaran, Solid State Ionics 161 (2003) 197.
[13] S.T. Myung, S. Komaba, N. Kumagai, Solid State Ionics 170 (2004) 139.
[14] L. Zhang, D. Li, X. Wang, H. Noguchi, M. Yoshio, Mater. Lett. 59 (2005) 2693.
[15] P.S. Whitfield, S. Niketic, I.D. Davidson, J. Power Sources 146 (2005) 617.
[16] F. Izumi, Nippon Kesssho Gakkai Shi 27 (1985) 23.
[17] Z. Lu, L.Y. Beaulieu, R.A. Donaberger, C.L. Thomas, J.R. Dahn, J. Electrochem. Soc. 149 (2002) A778.
[18] R.D. Shannon, Acta Crystallogr. A 32 (1976) 751.
[19] H. Noguchi, L. Zhang, M. Yoshio, Abstract of 41st Battery Symposium in Japan, Nagoya, 2000, p. 388.
[20] L. Zhang, T. Muta, H. Noguchi, X. Wang, M. Zhou, M. Yoshio, Electrochim. Acta 49 (2004) 3305.